

IMECE2007-43051

MODELING AND EXPERIMENTAL STUDY OF A BIOLOGY-INSPIRED DIRECTIONAL MICROPHONE

Zhong Chen, Alexander Lacher, and Miao Yu
Department of Mechanical Engineering
University of Maryland, College Park, MD, 20742

ABSTRACT

In this paper, a novel design of a biology-inspired directional microphone is presented. This microphone consists of two clamped circular diaphragms, which are mechanically coupled by a connecting bridge that is pivoted at its center. A mechanics based model is constructed to determine the response of the proposed directional microphone to sound incident from an arbitrary direction. The simulation results show that the proposed biology-inspired miniature directional microphone provides a remarkable amplification of the time delay associated with the sound induced diaphragm responses. Different parameters such as coupling bridge stiffness and damping factor are studied to evaluate the performance of the directional microphone. Preliminary experimental results are presented and compared with model predictions. The analyses and results are expected to be helpful for realizing an optimal version of the biology-inspired miniature directional microphone with high accuracy and localization capability for various applications.

1 INTRODUCTION

Sound source localization is important for many applications, including hearing aids, robot navigation, and sensor networks (e.g., Gay and Benesty, 2000). In existing sound source localization methods, like in humans and most other vertebrates, a time delay estimation based locator is widely used to calculate the sound-source azimuth relative to the microphone array, in particular, to realize real time localization with digital systems. In applying these methods, one concern is that noise and reverberation can seriously degrade a microphone's reception. For this reason, an accurate determination of time delay between microphones is very important for accurate sound direction detection. In addition, the microphones need to be located far enough from each other, so that the differences between the arrival times of the sound

field at these microphones can be detected. This poses a fundamental challenge to the miniaturization of directional acoustic sensor systems. However, in some small insects, the auditory receptors are forcibly set close to each other. In these cases, the interaural differences are often too small to be useful as directional cues, if they are to be processed by the nervous system. Such ears can be found in the parasitoid fly *Ormia Ochracea*, which shows a remarkable ability to locate a sound source both in nature and in the laboratory (Cade, 1975, 1996; Walker, 1993; Mason, Oshinsky, and Hoy, 2001). With a separation of only 520 μm between the ears, *Ormia* has an interaural time difference (ITD) of 1.45 μs and an interaural intensity difference (IID) of less than 1 dB. The fly *Ormia* can detect extremely small changes (less than 2 degrees) in the incident sound field direction.

In recent years, extensive studies have been performed on the fly *Ormia Ochracea*'s auditory organ. It was found that the interaural difference in fly ear response is greatly amplified due to the mechanical coupling between the ears' motions, which is provided by a cuticular structure that joins the two membranes and pivots about its center. Miles, Robert, and Hoy (1995) proposed a two-degree-of-freedom (DOF) mechanical model to illustrate the mechanism that is used by the fly ears to amplify interaural differences. In this model, the two ears are modeled as two spring-mass systems coupled by another torsion spring, and the motions of the fly ears are described as a combination of a rocking mode and a bending mode. This two DOF model was also experimentally verified. Based on these studies, some miniature biology-inspired directional microphone diaphragms were designed and fabricated (Yoo, Su, Miles, and Tien, 2001; Saito, Ono, and Ando, 2002; Miles and Hoy, 2006). Preliminary test results show that the two DOF model can explain the experimental data.

Although the simplified two DOF model can provide an explanation for the exceptional directional hearing ability of the fly *Ormia*, it is not very helpful for designing a biology-inspired directional microphone. Noting that the auditory organs of the fly *Ormia* include two diaphragms (tympanal

membranes) connected by an intertympanal bridge, it is necessary to use a distributed-parameter model to obtain a more complete understanding of the vibratory motions of the diaphragms-bridge system. This is supported by experiments carried out with the actual fly ears, which point to the presence of diaphragm vibratory modes (Robert, Read, and Hoy, 1998). Hence, to fully realize the potential of the fly *Ormia*'s directional hearing mechanisms, a more sophisticated model that can capture the essential dynamics of the mechanical structure (two mechanically coupled diaphragms) is needed. In the authors' previous work, a design of the biology-inspired miniature directional microphone was presented and an ANSYS model was used to evaluate the capability for sound incident angle detection (Chen and Yu, 2007). This model takes into account the coupling between the two diaphragms as well as the effect of the air cavity below a diaphragm. However, the ANSYS model is not sufficient to fully understand the physics of the system and carry out an optimal design.

In this article, a mechanics based model of a fly ear inspired miniature directional microphone is presented. Numerical simulations are carried out to study various design parameters such as the stiffness and damping factor of the coupling bridge (intertympanal bridge). Results obtained from preliminary experiments are also presented and compared with model predictions.

2 ACOUSTIC LOCALIZATION BY AZIMUTH CALCULATION

In order to locate the sound source acoustically, one method is to identify the azimuth angle of sound source relative to the directional microphone sensors as shown in Fig. 1. For a far field sound source, it can be assumed that plane waves are incident on each microphone diaphragm. Here, by "far field", it is meant that the distance between the sound source and each microphone is many times the square of sound source

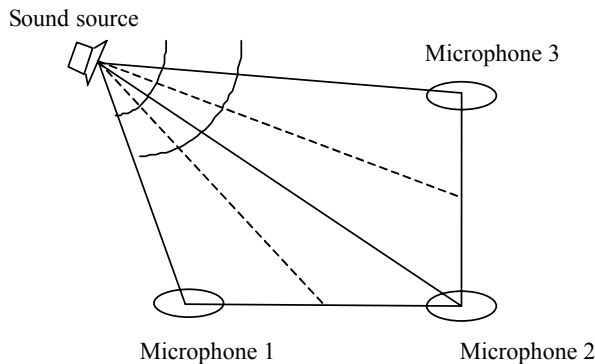


Figure 1. Schematic of sound source localization by azimuth calculation.

dimension divided by the sound wave length (Gay and Benesty, 2000). Based on this assumption, the azimuth angle φ of sound source relative to each microphone (the two microphones will be referred to as the left microphone and the right microphone) can be calculated from

$$\varphi = \arcsin(c\tau / d) \quad (1)$$

where c is the sound speed, d is the distance between two microphones, and τ is the time delay in the sound arriving at the two different microphone locations. If the two microphone diaphragms are not coupled, it follows that the time delay associated can be determined as

$$\tau = d \sin \varphi / c \quad (2)$$

where φ is the sound incident azimuth angle.

In a general case, the time delay τ between the sound waves arriving at left and right microphones can be calculated by finding the time corresponding to the maximum value of the cross-correlation of the displacement responses of two single microphones; that is

$$\tau = \arg \text{Max} \left(\int w_l(t + \tau) \times w_r(t) dt \right) \quad (3)$$

where w_l is the displacement response at the center of left microphone, and w_r is the displacement response at the center of right microphone. The corresponding phase delay ψ is calculated from

$$\psi = 2\pi f \tau \quad (4)$$

where f is the sound wave frequency.

3 ANALYTICAL MODEL DEVELOPMENT

As shown in Fig. 2, the proposed directional microphone consists of two clamped circular diaphragms. A bridge, which is pivoted about its center, connects the two diaphragm centers.

To develop a first generation model, the mass of the connecting bridge is neglected and it is modeled as having spring-damper effect on each of the diaphragms. The associated

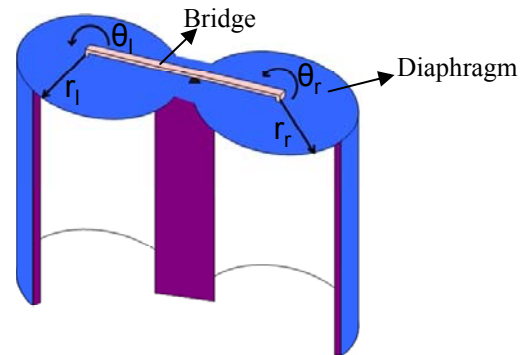


Figure 2. Structure of biology-inspired directional microphone.

spring stiffness is labeled as k and the associated viscous damping coefficient is labeled as c_a . Choosing polar coordinates systems with origins at the respective diaphragm centers, the equations governing the open domains of the left and right diaphragms shown in Fig. 2 can be written as

$$\begin{aligned} & D\nabla^4 w_l + \gamma \dot{w}_l + \rho h \ddot{w}_l \\ &= f_l - \frac{k\delta(r_l)}{\pi_l} \left[w_l(0, \theta_l, t) + w_r(0, \theta_r, t) \right] \\ & - \frac{c_a \delta(r_l)}{\pi_l} \left[\dot{w}_l(0, \theta_l, t) + \dot{w}_r(0, \theta_r, t) \right] \end{aligned} \quad (5)$$

and

$$\begin{aligned} & D\nabla^4 w_r + \gamma \dot{w}_r + \rho h \ddot{w}_r \\ &= f_r - \frac{k\delta(r_r)}{\pi_r} \left[w_l(0, \theta_l, t) + w_r(0, \theta_r, t) \right] \\ & - \frac{c_a \delta(r_r)}{\pi_r} \left[\dot{w}_l(0, \theta_l, t) + \dot{w}_r(0, \theta_r, t) \right] \end{aligned} \quad (6)$$

where $w_l(r_l, \theta_l, t)$ denotes the displacement of the left diaphragm and $w_r(r_r, \theta_r, t)$ denotes the displacement of the right diaphragm. Further, $D = Eh^3/12(1-\nu^2)$, where E , ν , γ , ρ and h denote the diaphragm Young's modulus, Poisson's ratio, damping coefficient, density, and thickness, respectively. The forces $f_l(r_l, \theta_l, t)$ and $f_r(r_r, \theta_r, t)$ correspond to the pressure fields applied on left and right diaphragms, respectively. The delta function δ is used to locate the force due to the bridge at each diaphragm center.

In terms of boundary conditions, the left and right diaphragms are assumed to be clamped along their respective edges; that is, at $r_l = a$, where a is the diaphragm radius, $w_l = 0$ & $\partial w_l / \partial r_l = 0$; and at $r_r = a$, $w_r = 0$ & $\partial w_r / \partial r_r = 0$.

4 MODEL PREDICTIONS AND DISCUSSION

4.1 Vibration mode analysis

In the simulations, following earlier work (Chen and Yu, 2007), the material properties used listed in Table 1 are used. The radius of each circular diaphragm is assumed to be 0.3 mm and the thickness of the diaphragm is assumed to be 1 μ m. The Table 1. Material properties used in the simulations.

Material	E (GPa)	ρ (kg/m ³)	Poisson's ratio
Polyimide (diaphragm)	7.5	1200	0.35

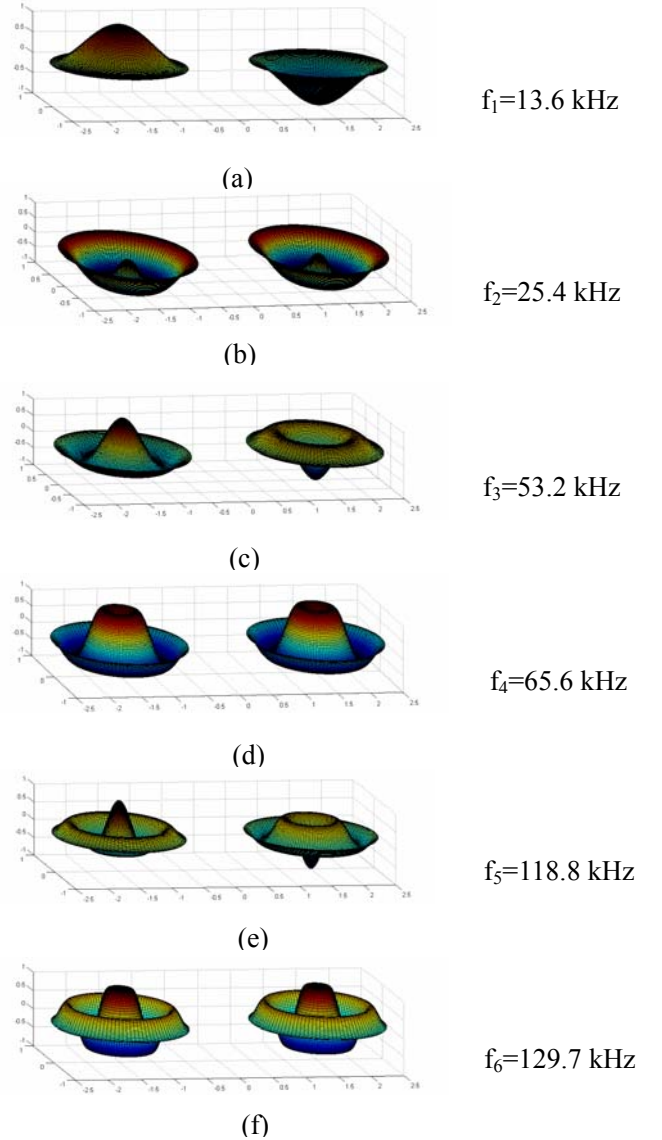


Figure 3. Different vibration modes of the biology-inspired miniature directional microphone diaphragm with the bridge stiffness of 0.6 units: (a) first rocking mode, (b) first bending mode, (c) second rocking mode, (d) second bending mode, (e) third rocking mode, and (f) third bending mode.

distance between the centers of the two diaphragms is assumed to be 0.8 mm.

Unlike the two DOF model proposed by Miles *et al.* (1995), which only predicts a rocking mode and a bending mode, the system considered here has an infinite number of vibration modes. In Fig. 3 (a)-(f), the first three rocking modes and three bending modes are shown. It is expected that

considering all these rocking modes and bending modes will be helpful for obtaining a more accurate picture of the sensor performance.

4.2 Parametric studies

As seen from Eqs. (5) and (6) of the model, the strength of coupling between the motions of the two clamped diaphragms is determined by the values of bridge stiffness k and damping coefficient c_d . In terms of the bridge stiffness, the coupling bridge is characterized as “soft”, “medium” and “hard” bridges, as given in Table 2.

For different bridge stiffness and damping coefficients, the time delay and phase delay between the responses of the two diaphragm centers subject to planar sound waves incident from 45 degrees and 60 degrees are studied as a function of the sound source frequency. The results obtained are shown in Fig. 4-6. The phase delay response is calculated from the time delay by using Eq. (4). These results are compared with those obtained for two separate microphones without coupling. In the case of two closely spaced but different microphones, the results obtained for an angle of incidence of 45 degrees are not much different from those obtained for an angle of incidence of 60 degrees. So, only the results obtained for the 45 degrees case is shown.

Similar to the results obtained previously from the two DOF model and the ANSYS model of the authors’ previous work, the system first rocking frequency is determined by the diaphragm properties and the first bending frequency is determined by the properties of both the diaphragm and the connecting bridge. From Figs. 4-6, it can be seen clearly that, for a system with a small damping factor, in all three coupled cases, the system has nearly the same first rocking frequency, which is around 14 kHz. As shown in Fig. 4(a), at the system first rocking frequency, the phase delay of the motions at the center of two diaphragms achieves the maximum value of 180 degrees. When the sound excitation frequency passes the first rocking frequency, a jump of 360 degrees appears in phase delay response because of the sign change when calculating the time corresponding to the maximum value of cross correlation between the two diaphragm center responses. As to the system first bending frequency, it changes with different stiffness values of the connecting bridge. The harder, the connecting bridge, the higher, the system first bending frequency. At the system first bending frequency, the phase delay between responses of the two diaphragm centers takes the value of

Table 2. Bridge stiffness values.

Structure	Diaphragm	Soft bridge	Medium bridge	Hard bridge
Stiffness (N/m)	0.388	0.1	0.6	12

0°. Since, the sound incident angle is determined by calculating the time delay response and the signs of time delay values are opposite when the sound is incident from the left side and the right side relative to the directional microphone, the frequency range below the first rocking frequency is used so that one can easily detect from which side the sound is incident by only checking the sign of time delay. In this study, the phase delay and the time delay response around this frequency range are considered.

In Fig. 4, for the “soft bridge”, when the sound excitation frequency is not very high compared with the system first rocking frequency, it is shown that the time delay is not significantly amplified compared to those obtained with two separate microphones (only about two times of amplification). This is due to the fact that a soft bridge cannot provide strong coupling between the two diaphragm motions. On the other hand, if the connecting bridge is too hard, as shown in Fig. 5, which is very much like a rigid bridge, the time delay is amplified to many times of the response of two separate microphones. The corresponding phase delay is always close to 180°, which is the maximum achievable phase delay. Although the time delay and corresponding phase delay are amplified most in this case, the problem is that it is almost impossible to

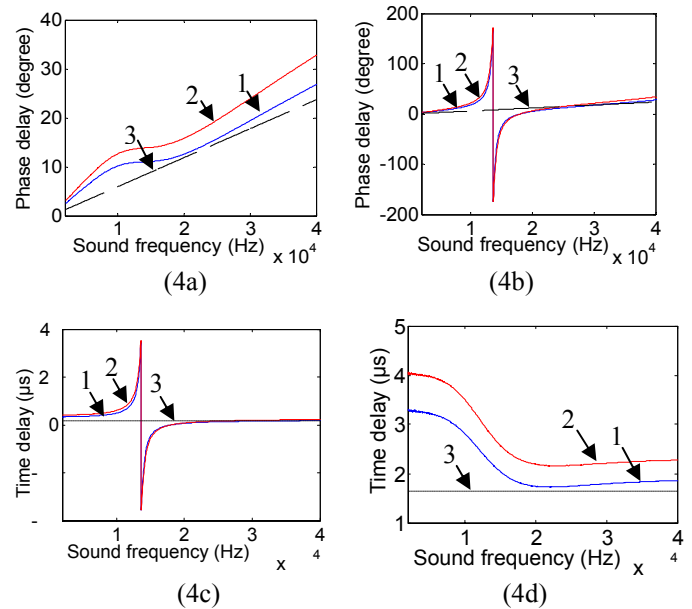


Figure 4. Phase delay and time delay responses for system with the soft bridge of Table 2 compared with those of the corresponding uncoupled microphone pair: (a) Phase delay for system with damping factor of 0.01, (b) Phase delay for system with damping factor ζ of 0.6, (c) Time delay for system with damping factor of 0.01, (d) Time delay for system with damping factor of 0.6. The graphs labeled 1, 2, and 3 correspond to the incident angle $\alpha=45^\circ$ for the coupled microphone pair, the incident angle $\alpha=60^\circ$ for the coupled microphone pair, and the incident angle $\alpha=45^\circ$ for the uncoupled microphone pair, respectively.

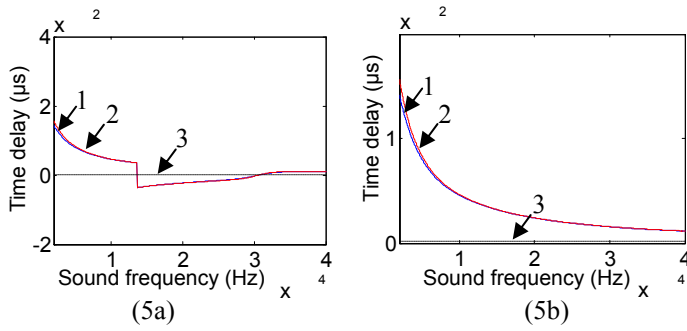


Figure 5. Time delay responses for system with the hard bridge of Table 2 compared with those of the corresponding uncoupled microphone pair: (a) damping factor $\zeta=0.01$ and (b) damping factor $\zeta=0.6$. The graphs labeled 1, 2, and 3 correspond to the incident angle $\alpha=45^\circ$ for the coupled microphone pair, the incident angle $\alpha=60^\circ$ for the coupled microphone pair, and the incident angle $\alpha=45^\circ$ for the uncoupled microphone pair, respectively.

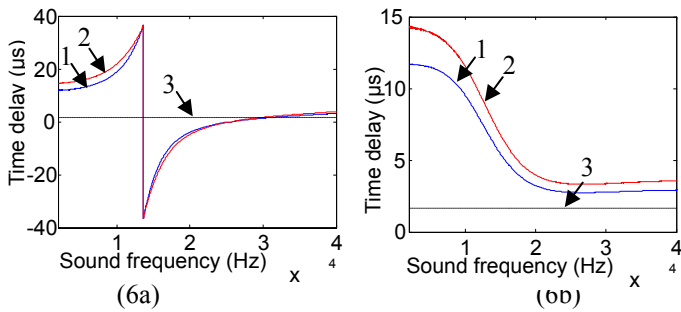


Figure 6. Time delay responses for system with the medium bridge of Table 2 compared with those of the corresponding uncoupled microphone pair: (a) damping factor $\zeta=0.01$ and (b) damping factor $\zeta=0.6$. The graphs labeled 1, 2, and 3 correspond to the incident angle $\alpha=45^\circ$ for the coupled microphone pair, the incident angle $\alpha=60^\circ$ for the coupled microphone pair, and the incident angle $\alpha=45^\circ$ for the uncoupled microphone pair, respectively.

distinguish the sound waves from different incident angles, since the time delays are very close to each other for different incident angles. This means that a microphone that has a stiff coupling bridge will have a very small resolution to detect the sound wave directions; in other words, the minimum audible angle (MAA) is very big. This problem can be addressed by using a medium connecting bridge. As shown in Fig. 6, when the sound excitation frequency is not close to the system first rocking frequency, it is seen that the time delay is amplified by more than 7 times compared to the uncoupled case. Further, the time delays associated with sound field incident from 45° and 60° degrees are easily distinguishable. Thus, both big amplification of the time delay and small MAA can be achieved. The respective diaphragm responses are shown in Fig. 7.

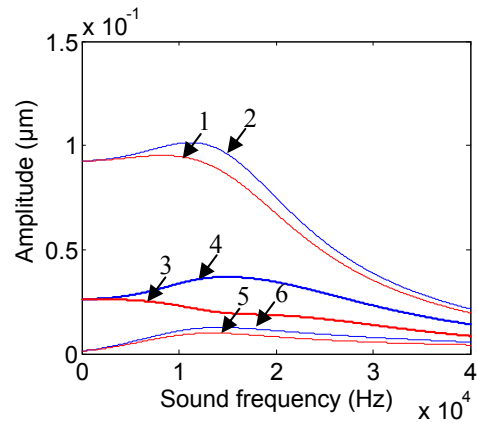


Figure 7. Displacement amplitude response versus excitation frequency for a diaphragm damping factor $\zeta=0.6$ and sound incidence angle of 45 degrees. Graphs labeled 1, 3, and 5 represent the responses of the left diaphragm center, and graphs 2, 4, and 6 represent the responses of the right diaphragm center. Graphs 1&2, 3&4, and 5&6 are obtained for a soft bridge, medium bridge, and hard bridge, respectively.

5 A POSSIBLE DESIGN PROCEDURE

Here, a formulation is provided to design a directional microphone for a specific sound frequency f_0 , minimum angle of incidence to be detected, and minimum pressure p_0 to be detected. Let the minimum incident angle difference detectable by the biology-inspired directional microphone be 1 degree. Then, the design can be carried out according to

$$\text{Maximize: Time_delay}(k, c_a) \text{ at } \alpha=1, f=f_0 \quad (7)$$

$$\text{Maximize: } d[\text{Time_delay}(k, c_a)]/d\alpha \text{ at } \alpha=90, f=f_0 \quad (8)$$

subject to the requirements

$$\text{Time_delay}(k, c_a) > T_0 \text{ at } \alpha=1, f=f_0 \quad (9)$$

$$\text{Amplitude}(k, c_a) > D_0 \text{ at } \alpha=1, f=f_0, p=p_0 \quad (10)$$

where α is the sound incident angle in degrees, k is the bridge stiffness, and c_a is the bridge damping factor. Note that in Eq. 8, the derivative of the time delay is with respect to the incident angle is maximized for angle $\alpha=90$ because the derivative is minimum when incident angle is equal to 90° . Further studies are currently being conducted to study this formulation.

6 PRELIMINARY EXPERIMENTAL RESULTS AND COMPARISON WITH MODEL PREDICTIONS

To investigate the performance of the proposed biology-inspired directional microphone, a setup was constructed as shown in Fig. 9(a). The bridge is glued to the diaphragm center and the supporting point at its center with epoxy. The diaphragm and bridge material properties are as listed in Table 3. The diaphragm has a diameter of 3.8mm and a thickness of 40 μ m. The length, width and thickness of the bridge are 25.4 mm, 1.2 mm, and 0.2 mm, respectively. A low coherence Fabry-Perot interferometer based fiber optic system with very high sensitivity was used to measure the vibrations of these two large scale microphone diaphragms. A loudspeaker was used as sound source to produce sound signals of different frequencies. The biology-inspired directional microphone was placed far away from the speaker and the sound incident angle is changed by moving the speaker around the biology-inspired directional microphone. The schematic of the experiment setup is shown in Fig. 9(b).

Table 3. Diaphragm and bridge material properties.

	Material	E(GPa)	Poisson's ratio	Density (kg/m ³)
Diaphragm	Mylar	3.45	0.41	1290
Bridge	Brass	115	0.31	8400

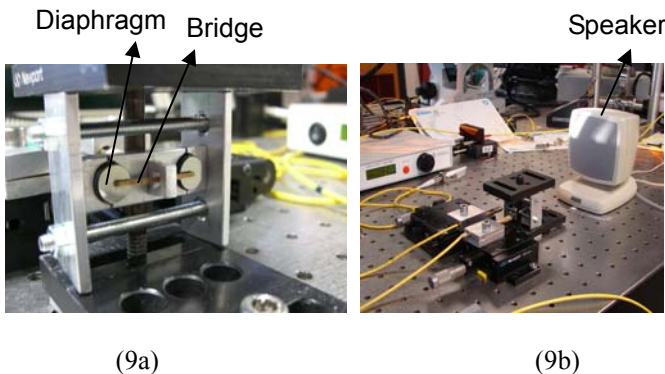


Figure 9. Preliminary experiment setup: (a) biology-inspired directional microphone in large scale and (b) arrangement showing the sound source.

In Fig. 10, both the model predictions and experimental results are shown for the phase delay response in the coupled microphone pair and uncoupled microphone pair cases. The

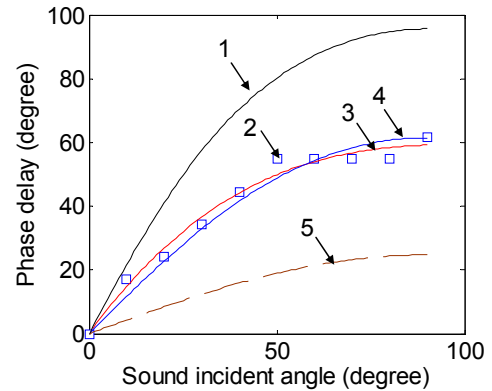


Figure 10. Comparison of experimental results with model predictions: The graph labeled 1 corresponds to the model prediction for the coupled microphone pair case with $k=67$ units, and the graph labeled 4 corresponds to the model predictions for the coupled microphone case with $k=27$ units. The legend 2 is used to refer to the experimental data through which the graph labeled 3 is fitted. The graph labeled 5 corresponds to the model prediction for the uncoupled microphone pair case.

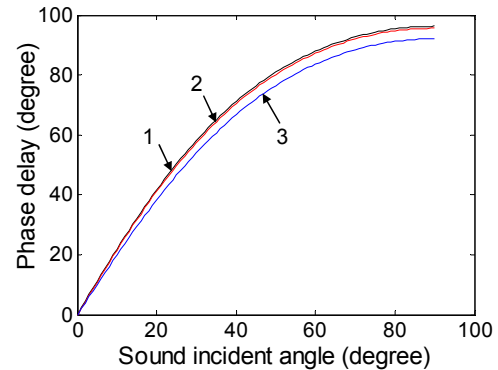


Figure 11. Model predictions for phase delay versus sound incident angle for different damping factors. The graphs labeled 1, 2, and 3 correspond to damping factors of 0.05, 0.2, and 0.5, respectively.

excitation frequency is 1 kHz. A damping factor of 0.2 is used in the simulations for each of the diaphragms and the bridge. As seen from the measured data, the biology-inspired directional microphone shows around three times amplification of the phase delay obtained in the uncoupled case. The measured phase delay amplification is lower than the amplification predicted for a bridge stiffness value of 67 units. However, when this value is dropped to 27 units, a better comparison between experimental results and model predictions (graph labeled 4 in Fig. 10) is seen. When the damping factor is changed, the model predictions vary as shown in Fig. 11. As can be seen, with different damping

factors, the phase delay response does not change much since the considered excitation frequency of 1 kHz is very low compared to the first rocking frequency of the fabricated biology-inspired directional microphone, which is around 2.3 kHz.

CONCLUDING REMARKS

In this article, a mechanics model of a biology-inspired miniature directional microphone has been presented. The simulation results show that the proposed biology-inspired miniature directional microphone has appealing performance characteristics. In addition the constructed model allows one to study the influence of parameters such as the bridge stiffness and bridge damping coefficient in the coupled microphone case. Currently, additional work is being carried out to characterize the coupling bridge properties as well as to establish a design formulation.

ACKNOWLEDGEMENTS

The authors gratefully acknowledge the support received from the U.S. National Science Foundation (NSF) under the award CMMI 0644914 and Oak Ridge Associated Universities under the University of Maryland contract ATS-01-431662.

REFERENCES

- Cade, W. H., 1975, "Acoustically orienting parasitoids: fly phonotaxis to cricket song," *Science*, Vol. 190, pp. 1312-1313.
- Walker, T. J., 1993, "Phonotaxis in female *Ormia Ochracea* (Diptera: Tachinidae), a parasitoid of field crickets," *Journal of Insect Behavior*, Vol. 6, pp. 389-410.
- Robert, D., Read, M. P., and Hoy R. R., 1994, "The tympanal hearing organ of the parasitoid fly *Ormia ochracea* (Diptera, Tachinidae, Ormiini), *Cell Tissue Res*, Vol.275, pp. 63-78.
- Miles, R. N., Robert, D., and Hoy, R. R., 1995, "Mechanically coupled ears for directional hearing in the parasitoid fly *ormia ochracea*," *Journal of the Acoustical Society of America*, Vol. 98(6), pp. 3059-3070.
- Cade, W. H., Ciceran, M., and Murray, A. M., 1996, "Temporal patterns of parasitoid fly (*Ormia Ochracea*) attraction to field cricket song (*Gryllus integer*)," *Canadian Journal of Zoology*, Vol. 74, pp. 393-395.
- Robert, D., Miles, R. N., and Hoy, R. R., 1998, "Tympanal mechanics in the parasitoid fly *ormia ochracea*: intertympanal coupling during mechanical vibration," *Journal of Comparative Physiology A*, Vol. 183, pp. 443-452.
- Gay, S. L. and Benesty J., 2000, *Acoustic Signal Processing for Telecommunication*, Kluwer Academic, Boston.
- Mason, A. C., Oshinsky, M. L., and Hoy, R. R., 2001, "Hyperacute directional hearing in a microscale auditory system," *Nature*, Vol. 410, pp. 686-690.
- Yoo, K., Su, Q., Miles, R. N., and Tien, N. C., 2001, "Biomimetic direction-sensitive micromachined diaphragm for

ultrasonic transducers," *IEEE Ultrasonics Symposium*, pp. 887-890.

Saito, A., Ono, N., and Ando, S., 2002, "Micro gimbal diaphragm for sound source localization with mimicking *ormia ochracea*," *SICE*, Osaka pp. 2159-2162.

Popper, A. N. and Fay, R. R., 2005, "Sound Source Localization," Springer, New York.

Miles, R. N. and Hoy, R. R., 2006, "The development of a biologically-inspired directional microphone for hearing aids," *Audiology & Neurotology*, Vol. 11, pp. 86-94.

Chen, Z and Yu, M., 2007, "Dynamic analysis of a biology-inspired miniature directional microphone," *The Proc. of SPIE*, Vol. 6523.

